# Wide-Band Compact Modeling of Spiral Inductors in RFICs

Daniel Melendy*, Pascale Francis**, Christoph Pichler**,
Kyuwoon Hwang**, Gopal Srinivasan**,Andreas Weisshaar*
* Department of Electrical and Computer Engineering
Oregon State University
Corvallis OR 97331-3211
**National Semiconductor Corporation
Santa Clara, CA 95052

*Abstract*— **A new wide-band compact modeling methodology for planar spiral inductors on lossy silicon substrate is presented. The new ideal lumped-element equivalent circuit model employs transformer loops in the series branch to include the effects of the frequency-dependent losses, in particular eddy-current loss in the bulk silicon substrate. A robust automated extraction procedure is employed to extract the element values of the new compact model. The new automated modeling methodology has been applied to a typical 1.5nH spiral fabricated on a low-resistivity CMOS substrate. The frequency-dependent series resistance and inductance as well as the quality factor obtained with the new wide-band model are in excellent agreement with the measured results over a 10GHz bandwidth.**

## I. Introduction

As RFIC applications more commonly reach frequencies in the 1-10GHz region, the demand for accurate wide-band compact models for on-chip spiral inductors has significantly increased. To give IC design engineers a real benefit, the compact model topology should use a minimum number of ideal lumped elements while offering a maximum amount of modeling flexibility. Furthermore, having a robust automated extraction procedure is desirable to reliably and efficiently extract the model parameters for a given spiral inductor design. Low cost CMOS processes, in particular, demand a flexible compact model topology due to a variety of loss mechanisms present at higher frequencies. These loss mechanisms, which include eddy-current losses in the substrate as well as losses due to the conductor skin and proximity effects, may have an especially negative impact on the performance of on-chip spiral inductors.

The most commonly used compact spiral inductor model is the standard "9-element" $\pi$-model (e.g. [1], [2]). The series branch of the 9-element model consists of a series combination of an inductor and a resistor together with a parallel-connected capacitor, which may be thought of as representing the capacitive coupling to the underpass as well as between the turns of the spiral inductor. While this model can be used over a wide frequency range for spiral inductors on low-loss substrates such as high-resistivity silicon (HRS) or sapphire [3], it does not properly model wide-band eddy-current loss in the silicon substrate for medium to heavily doped silicon processes. In the more heavily doped silicon processes, the series branch in the $\pi$-model of a spiral inductor may exhibit a significant frequency dependence in the series resistance $R(\omega)$ and inductance $L(\omega)$. Eddy-current loss in the substrate, which is the dominant ac loss effect in low resistivity substrates [4], causes $L(\omega)$ to decrease and $R(\omega)$ to increase with increasing frequency. Below the self-resonant frequency of the spiral, the series branch of the 9-element model exhibits an increasing inductance and increasing resistance as a function of frequency. Without the coupling capacitor, the series R and L of the 9-element model have no frequency dependence. These trends limit the usefulness of the 9-element model as a wide-band compact model for spiral inductors on low resistivity substrates.

This paper presents a new methodology for wide-band compact modeling including automated parameter extraction for planar spiral inductors on lossy silicon substrate. The compact model achieves high accuracy over a wide frequency range by using transformer loops (similar to the substrate current loops used in the equivalent circuit model for on-chip interconnects [4],[5]) to model the effects of frequency-dependent losses in spiral inductors, in particular eddy-current loss in low-resistivity silicon substrates [6]. The values of the ideal elements of the wide-band equivalent circuit model are determined from two-port S-parameters using a robust automated extraction procedure based on a least-squares fitting algorithm.

## II. Wide-Band Equivalent Circuit Model

Figure 1 shows the wide-band compact model for spiral inductors. The inductance $L_{dc}$ and resistance $R_{dc}$ in the series branch represent the spiral inductor's series resistance and inductance at the low frequency limit. The coupling capacitance, commonly used in the 9-element model, has been neglected to obtain the correct trends for the series $L(\omega)$ and $R(\omega)$. The inductance $L_{s_i}$ and resistance $R_{s_i}$ simulate the ith transformer loop to ac-



0-7803-7239-5/02/$10.00 © 2002 IEEE

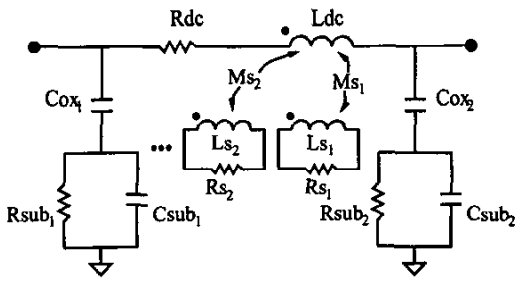


Fig. 1. Wide-band compact equivalent circuit model for spiral inductors on lossy substrates.

count for the frequency-dependent losses. The mutual inductances $M_{s_i}$ between $L_{s_i}$ and $L_{dc}$ can be thought of representing the inductive coupling between the spiral metallization and the semiconducting substrate. The impedance of the series branch with transformer loops is given by [5]:

$$Z_{series}(\omega) = R_{dc} + j\omega L_{dc} - \sum_{i=1}^{N} \frac{M_{s_i}(j\omega)^2}{R_{s_i} + j\omega L_{s_i}} \qquad (1)$$

where $N$ is the number of transformer loops. With only a single loop, the series circuit is effectively a simple transformer with a resistive load. Each additional transformer loop adds an extra term to the summation in (1), which allows for more variability in the frequency response. At low frequencies the transformer loops are weakly coupled to $L_{dc}$ such that the frequency response of the series circuit is dominated by $L_{dc}$ and $R_{dc}$.

The standard $C$-$GC$ topology consisting of ideal $G$ and $C$ elements is used for the shunt branches in the $\pi$-configuration of the wide-band compact model. In certain cases, increased accuracy of the overall model can be obtained by using a more general shunt circuit. This can be realized by adding one or more parallel $G$-$C$ combinations in series with the basic $C$-$GC$ circuit. The input impedance of these augmented circuits is:

$$Z_{shunt_k}(\omega) = \frac{1}{j\omega C_{ox_k}} + \sum_{i=1}^{N} \frac{1}{G_{sub_{k,i}} + j\omega C_{sub_{k,i}}} \qquad (2)$$

where $N$ is the total number of $G-C$ combinations in the shunt circuit and k is the port number.

## III. Extraction Procedure

An important consideration in developing compact models is the need for a fast and accurate means of extracting the component values. Typically, compact models, such as the 9-element model, are extracted using a time-consuming optimizer. Because optimizers involve an iterative solution process they can be prone to convergence problems, depending on the initial values supplied by the user. The optimizer may converge to a "local minimum" or possibly never reach convergence. To avoid these problems with the more complex transformer loop model, we have developed a robust CAD-oriented extraction methodology using a least-squares (LS) fitting procedure. Because of the large number of frequency points and limited number of components, the LS fitting procedure involves the solution of an overdetermined system of equations. Note that this extraction approach is feasible because of the simple mapping between the coefficients of the resulting rational polynomial and the component values in the wide-band compact model.

As (1) and (2) show, both the series and shunt impedance functions include summations of single pole terms which can be rewritten as rational polynomial functions of $j\omega$. To take advantage of the rational polynomial form, Cauchy's method [7],[8] is used to extract the component values involved in the summations. In this formulation $L_{s_i}$, the loop inductances, are all arbitrarily scaled to $1\mu H$. To illustrate the extraction procedure, the main steps are described for the series impedance branch. The shunt circuit extraction is similar and the main differences will be explained.

The series impedance can be directly obtained from the measured $Y_{12}$ admittance parameter as

$$Z_{series}(\omega) = \frac{-1}{Y_{12}(\omega)} = R(\omega) + j\omega L(\omega) \qquad (3)$$

The dc values of $L(\omega)$ and $R(\omega)$ can be found by separating the measured data, according to (3), into the resistive and inductive parts and extracting the low frequency asymptotes of both curves. After obtaining $R_{dc}$ and $L_{dc}$, the remaining unknowns are isolated by rearranging (1):

$$T(jw) =: \frac{R_{dc} + j\omega L_{dc} - Z_{series}(\omega)}{(j\omega)^2} = \sum_{i=1}^{N} \frac{M_{s_i}}{R_{s_i} + j\omega L_{s_i}} \qquad (4)$$

Eq. 4 shows that the only remaining terms are due to the transformer loops and are contained in a summation of single pole functions. This summation can be rewritten as a rational polynomial in $j\omega$

$$T(jw) = \frac{a_0 + a_1(\omega) + \cdots + a_{n-1}(j\omega)^{n-1}}{b_0 + b_1(j\omega) + \cdots + b_n(j\omega)^n} = \frac{N(j\omega)}{D(j\omega)} \qquad (5)$$

Rewriting (5) and applying to each frequency point $\omega_m$ $(m = 1, 2, \ldots, M)$ results in a set of $M$ complex equations of the form

$$T(j\omega_m) * D(j\omega_m) - N(j\omega_m) = 0 \qquad (6)$$

The total number of coefficients in the rational polynomial is 3 or 5 for the single and double transformer loop models, respectively, while the number of frequency points is on the order of 100 in the example shown in this

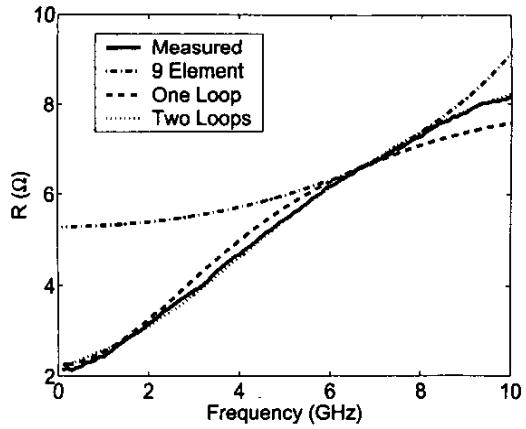


Fig. 2. Series $R(\omega)$ for measurements, single-loop, double-loop, and the 9-element model.

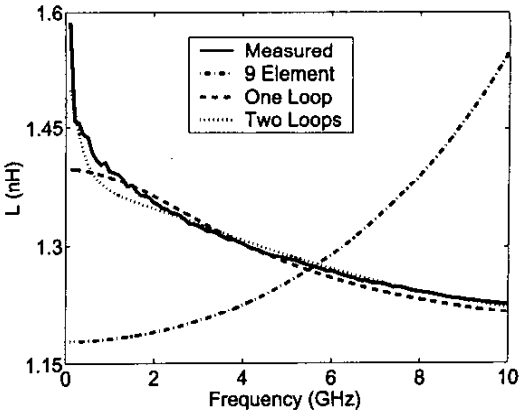


Fig. 3. Series $L(\omega)$ for measurements, single-loop, double-loop, and the 9-element model.

paper. The resulting over-determined system is solved directly using an eigenvalue equation approach.

The impedance function of the shunt circuits is similar in form to that of the series branch circuit, as can be seen from (2). $C_{ox}$ can be extracted from the low frequency asymptote of the shunt impedance, and the impedance function is rearranged as follows:

$$Z_{shunt_k}(\omega) - \frac{1}{j\omega C_{ox_k}} = \sum_{i=1}^{N} \frac{1}{G_{sub_{k,i}} + j\omega C_{sub_{k,i}}} \quad (7)$$

This form directly leads to an extraction using Cauchy's method as explained above.

Because of the similarities in the impedance functions of the series and shunt circuits of the wide-band compact model, the same algorithm can be used to extract all three branches of the equivalent circuit model, which leads to a very compact and efficient extraction procedure. The extraction time for both the single and double loop models, with $C-GC$ or $C-GC-GC$ shunt circuits, typically is on the order of 10 seconds.

## IV. Results

To demonstrate the capabilities of the new wide-band compact modeling and extraction methodology, two equivalent circuits have been extracted from the measured two-port scattering parameters of a 4.5 turn 1.5nH spiral inductor. The spiral inductor was fabricated in a standard CMOS process with bulk substrate resistivity of about 0.015 Ω-cm and a 30 Ω-cm epi layer. The first compact model extracted uses only a single transformer loop, while the second model uses two transformer loops. Table I lists the extracted component values obtained with the automated extraction procedure described above. Both compact models use the same shunt circuit values so that all improvements from the single to the double-loop model can be attributed to the additional transformer loop. For comparison, a 9-element compact model has also been extracted from the measurements using an optimizer. The $R(\omega)$ and $L(\omega)$ curves for the extracted models are shown in Figs. 2 and 3 along with the measured results. The single loop model is able to match the broad-band $L(\omega)$ data with only 1.8 % rms error while the additional loop reduces this error to 1.0 %. The double loop model is much better at reproducing the $R(\omega)$ curve over the entire bandwidth with a rms error of 1.2 % as compared to 4.8 % with the single loop model. The double-loop compact model has the added benefit of allowing a much smaller error in $L(\omega)$ at the low frequency limit. This is possible because of the extra pole and zero in the impedance function that can be placed at a low frequency. In this case, the double-loop model has an error in the low frequency inductance of -5.5 % as opposed to -11.9 % with the single loop model. As Figs. 2 and 3 show, the 9-element model's trend of increasing inductance and resistance does not match well with the measured data and results in 12.9 % and 26.0 % rms error for $L(\omega)$ and $R(\omega)$, respectively.

To further illustrate the ability of the new compact model to accurately represent the spiral inductor over a broad frequency range, we have compared the quality factor $Q_{11}(\omega)$ of the new equivalent circuit models with the measured $Q_{11}(\omega)$. The quality factor $Q_{11}(\omega)$ is defined as:

$$Q_{11}(\omega) = \frac{Im(\frac{1}{Y_{11}(\omega)})}{Re(\frac{1}{Y_{11}(\omega)})} \quad (8)$$

Fig. 4 shows a comparison of $Q_{11}(\omega)$ for the complete single and double loop compact models, the 9-element model as well as the measured $Q_{11}(\omega)$. In this case the single loop model exhibits an rms error of 4.5 %, while the double loop model offers a much smaller rms error of 1.7 % over the entire 0.1 to 10GHz frequency range.

TABLE I

EXTRACTED EQUIVALENT CIRCUIT PARAMETERS FOR A 1.5NH SPIRAL

| Parameters | Single Loop Model | Double Loop Model | Parameters | Both Models |
|---|---|---|---|---|
| $R_{DC}$ | 2.2397 Ω | 2.0927 Ω | $C_{ox_1}$ | 35.781 fF |
| $L_{DC}$ | 1.3968 nH | 1.5113 nH | $C_{sub_{1,1}}$ | 191.59 fF |
| $R_{s_1}$ | 29470 Ω | 42427 Ω | $G_{sub_{1,1}}$ | 6.647 mS |
| $L_{s_1}$ | 1 μH | 1 μH | $C_{ox_2}$ | 30.999 fF |
| $M_{s_1}$ | 14.857 nH | 14.140 nH | $C_{sub_{2,1}}$ | 132.36 fF |
| $R_{s_2}$ | - | 2080.3 Ω | $G_{sub_{2,1}}$ | 9.144 mS |
| $L_{s_2}$ | - | 1 μH | - | - |
| $M_{s_2}$ | - | 12.328 nH | - | - |

The 9-element model, by comparison, offers 22.2 % rms error in its $Q_{11}(\omega)$ curve.

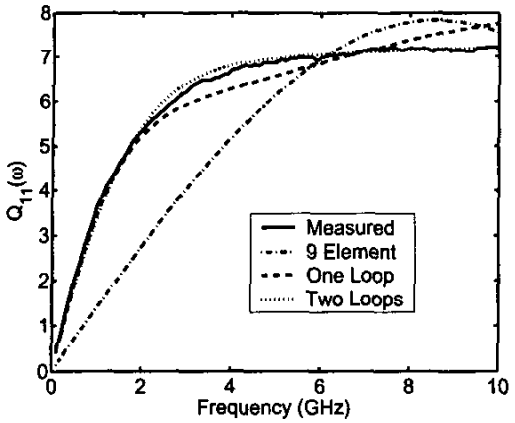


Fig. 4. Quality factor of measured spiral inductor compared with single-loop, double-loop, and 9-element models.

## V. CONCLUSION

A new methodology for wide-band compact modeling of spiral inductors on lossy silicon substrate has been presented. The modeling methodology consists of both a wide-band compact equivalent circuit model and an automated extraction procedure. The frequency-dependence in the series resistance and inductance of the spiral is modeled using coupled transformer loops, which mainly represent the effects of eddy-current loss in the semiconducting substrate. The automated extraction procedure is based on Cauchy's method and takes advantage of the simple mapping between the coefficients of the rational impedance functions and the equivalent circuit elements. The extracted transformer-loop model leads to a significant improvement in the ability to model the Q of a class of on-chip spiral inductors. The equivalent circuit models were tested in SpectreRF [9] and compared over the frequency range of 0.1 to 10 GHz with measurements of a 4.5 turn 1.5nH spiral inductor fabricated on a 0.015 Ω-cm process. The new methodology for wide-band compact model development for spiral inductors should be very useful in the design of RF and mixed-signal integrated circuits.

## REFERENCES


[1] J.R. Long, M.A. Copeland,"The Modeling, Design, and Characterization of Monolithic Inductors for Silicon RF IC's," *IEEE J. Solid-State Circuits*, vol. 32, pp.357-368, March 1997.

[2] S.S. Mohan, M.d.M. Hershensen, S.P. Boyd, and T.H. Lee,"Simple Accurate Expressions for Planar Spiral Inductors," *IEEE J. Solid-State Circuits*, vol. 34, pp. 1419-1424, Oct. 1999.

[3] J.N. Burghartz, D.C. Edelstein, K.A. Jenkins, and Y.H. Kwark,"Spiral Inductors and Transmission Lines in Silicon Technology Using Copper-Damascene Interconnects and Low-Loss Substrates," *IEEE Trans. Microwave Theory Tech.*, vol.45, Oct. 1997.

[4] J. Zheng, V.K. Tripathi, and A. Weisshaar,"Characterization and Modeling of Multiple Coupled On-Chip Interconnects on Silicon Substrate," *IEEE Trans. Microwave Theory Tech.*, vol.49, Oct. 2001.

[5] J. Zheng, Y.-C. Hahm, V.K. Tripathi, and A. Weisshaar, "CAD-Oriented Equivalent Circuit Modeling of On-Chip Interconnects on Lossy Silicon Substrate," *IEEE Trans. Microwave Theory Tech.*, vol.48, pp.1443-1451, Sept. 2000.

[6] D. Melendy et al., "A New Wide-Band Compact Model for Spiral Inductors in RFICs," submitted to *IEEE Electron Device Lett.*

[7] E.C.Levy, "Complex-curve fitting," *IRE Trans. Automatic Control*, vol. 4, pp.37-43, May 1959.

[8] K.L. Choi, N. Na, and M. Swaminathan, "Characterization of Embedded Passives Using Macromodels in LTCC Technology," *IEEE Trans. Comp. Packag., Manufact. Technol. B*, vol.21, pp.258-268, Aug. 1998.

[9] Cadence Design Systems Inc., San Jose, CA 95134, USA.